Biochimica et Biophysica Acta, 1070 (1991) 143–151

BBAMEM 75406

A neutron diffraction study of the influence of ions on phospholipid membrane interactions

S.A. Tatulian [1], V.I. Gordeliy [2], Albina E. Sokolova [1] and A.G. Syrykh [2]

[1] *Institute of Cytology, Academy of Sciences USSR, Leningrad (U.S.S.R.) and* [2] *Laboratory of Neutron Physics, Joint Institute for Nuclear Research, Dubna (U.S.S.R.)*

(Received 24 July 1991)

Key words: Dipalmitoylphosphatidylcholine; Lamellar structure; Neutron diffraction; Disjoining pressure

Neutron diffraction is used to examine the effects of Ca^{2+} and ClO_4^- ions on interactions and some structural features of dipalmitoylphosphatidylcholine membranes in both solid and fluid lamellar phases. The results are described within the framework of Derjaguin-Landau-Verwey-Overbeek (DLVO) theory with reference to electrostatic, van der Waals, and hydration components of disjoining pressure. The Hamaker constants are evaluated under equilibrium conditions. Addition of 100 mM $CaCl_2$ to the aqueous phase substantially increases the lamellar repeat spacing (d), which is interpreted in terms of adsorption of Ca^{2+} ions to bilayers followed by electrostatic repulsion between membranes. The rise of $NaClO_4$ concentration in the presence of 100 mM $CaCl_2$ leads to gradual decrease in d, evidently resulted from the diminution of Ca^{2+}-induced positive surface potential by both electrostatic screening and binding of ClO_4^- ions. In the absence of $CaCl_2$, elevation of $NaClO_4$ concentration to 100–300 mM drastically enhances the repeat spacing and then dramatically decreases d at about 1 M $NaClO_4$. Estimation of the hydration coefficients showed that the pronounced decrease of the repeat spacing at high $NaClO_4$ concentrations was resulted mainly from the (partial) disruption of the structure of intermembrane bound water by chaotropic ClO_4^- ions and subsequent decrease in hydration repulsive pressure. Moreover, in the case of solid membranes (20°C) high concentrations of ClO_4^- induced formation of interdigitated phase paralleled with marked reduction in bilayer thickness and corresponding increase in the effective cross-sectional area per lipid molecule.

Introduction

The intrinsic properties of lipid bilayers of cell plasma membranes are known to play decisive role in a number of physiologically important processes, such as intercellular adhesion and fusion [1–4]. These latter processes are controlled by the main components of intermembrane disjoining pressure, namely, the long-range electrodynamic (van der Waals) and electrostatic forces and short-range hydration (solvation, structural) forces [5–12] which may well be modulated by changes in the compositional-structural or other characteristics of the lipid bilayer [2–5,13–16]. Curtis and co-workers [15], for example, concluded that the alterations of cell adhesive properties induced by variations in the lipid composition of plasma membranes could be accounted for by changes in van der Waals forces (Hamaker constant). The dependence of cell adhesiveness on membrane fluidity was explained by thermotropic shifts in the surface potential of lipid bilayers, which in turn was mediated by adsorption of inorganic ions [3]. The fact that fluid bilayers are less adhesive as compared to solid membranes was alternatively interpreted in terms of more extensive hydration in the former case and increased hydration repulsion between fluid films [1,2,7,12,17,18] while the thermal undulations were also recognized to play a certain role [19–22].

The hydration forces are shown to dominate at intermembrane spacings $\leq$ 2–3 nm, increase exponentially with decreasing separation, and reach 10^7–10^{10} N/m^2 at the membrane surface [1,5,7,9–12,22,23]. Progressive increase in the hydration repulsive pressure between approaching membranes will obviously prevent molecular contacts. Therefore, the processes requiring tight intermembrane contact (e.g., membrane fusion) can only proceed when the membranes are (partially) dehydrated and hydration forces reduced [1,2,4]. As justly outlined by Parsegian and Rau [24],

Correspondence: S.A. Tatulian, Institute of Cytology, Academy of Sciences USSR, Tikhoretsky Avenue 4, Leningrad 194064, U.S.S.R.

"The force changes only if something else displaces water from the surface, and the displacement occurs only if the new species is more strongly attracted to the surface than is water". Some inorganic anions, such as SCN^- and ClO_4^-, could presumably be used as such species, since they were shown to bind to phospholipid bilayers quite strongly [25,26] and are potent water structure breakers by virtue of their chaotropic nature [27]. On the other hand, Ca^{2+} and other divalent cations adsorb to phospholipid membranes [3,6,17,18, 26,28,29] and give rise to strong electrostatic repulsion between zwitterionic lipids [6,17,28,29] and lower the hydration repulsion between acidic phospholipids [1,2,18].

These findings and considerations indicate that the understanding of the mechanisms of membrane adhesion requires detailed examination of lipid bilayer interactions under varying experimental conditions, concerning the temperature, ionic environment and others.

In this work, the effects of the adsorption of Ca^{2+} and ClO_4^- ions on interactions between dipalmitoylphosphatidylcholine (DPPC) membranes has been studied in a wide temperature range, including the solid-to-fluid phase transition of the lipid. It is shown that the influence of 100 mM Ca^{2+} or ≤ 300 mM ClO_4^- on membrane interactions is due to charge adsorption-induced electrostatic forces. Higher concentrations of ClO_4^- (≥ 1 M) decrease the hydration pressure owing to chaotropic effects and, in the case of solid membranes, induce the formation of interdigitated phase.

Materials and Methods

Materials. DPPC was obtained from Serva or Calbiochem (F.R.G.) or synthesized by one of us (A.E.S.). The purity of the lipid from all three sources checked by thin-layer- and gas-liquid-chromatography was higher than 99%. The salts NaCl, Na_2SO_4, $NaClO_4$, NaSCN, and $CaCl_2$ were purchased from Reachim (U.S.S.R.) and Tris(oxymethyl)aminomethan from Serva.

Experimental. To prepare the samples for neutron diffraction experiments, 10 mg of DPPC were weighed into thin quartz vials, then 50 μl of spectroscopic grade ethanol and 13.3 μl of buffered (10 mM Tris-HCl, pH 7.4) aqueous solution of appropriate ionic composition were added. The vials were thermostated at 60 °C for 3–4 h to homogenize the mixture and partially evaporate the ethanol and water. Then the samples were dried under progressively lowered pressure for ≈ 5 h, 20 μl of heavy water (^2H_2O) were added to the mixture of lipid and salt, the vials were sealed, thermostated at 60°C for 1 h, centrifuged at 4000 rpm for 1 h and kept at room temperature for 24 h. The final concentration of Tris-HCl in the samples was 6.65 mM (pH 7.4).

Using the molecular weights of DPPC and ^2H_2O as 734 and 20, respectively, and their densities at 20 °C (1.067 g/ml for DPPC [30] and 1.10533 g/ml for ^2H_2O [31]), the ^2H_2O/DPPC molar ratio in the samples is found to be ≈ 81. This water/lipid ratio was quite sufficient to allow the lipid to swell (see Refs. 5–7) which was confirmed by the fact that always excess water was present in the samples excepting the experiments when the water/lipid ratio was specially lowered to achieve the no-excess-water condition (see below).

The experiments were carried out on DN-2 neutron diffractometer with a one-dimensional position-sensitive detecter and IBR-2 pulse reactor of 2 MW power at the Laboratory of Neutron Physics, Joint Institute for Nuclear Research, Dubna. The pulse frequency was 5 Hz, and the integral neutron flux on the samples $1.3 \cdot 10^7$ cm^{-2} s^{-1}. The time-of-flight neutron diffraction technique was used. The Bragg angle between the incident and diffracted neutron beams was kept constant at $2\theta = 8°$ while the wavelength of the beam linearly varied from 0.12 to 2.0 nm during each pulse. The diffracted neutrons were counted by the detecter comprising 32 positional groups (0.5° between adjacent groups) and divided by 1024 time channels. The intensity (neutron counts) vs. time scans were accumulated and superposed, then translated into the scale of intensity vs. $\lambda/2 \sin\theta = d/n$ (here d is the repeat distance, λ the wavelength, and n the diffraction order). The first and second orders of diffraction peaks were recorded in 5 to 10 min (Fig. 1), and the lamellar repeat spacings deduced directly from the position of the first-order scattering peak with an accuracy of ± 0.15 nm. The reproducibility of the results of measurements under similar conditions was ± 0.2 nm.

Theoretical. The disjoining pressure between interacting lipid bilayers (P) is believed to be composed of a series of components, namely, the electrostatic (P_{es}), electrodynamic (P_{ed}), hydration (P_h) pressures, thermal-mechanical fluctuations (P_{fl}) and some other terms [1–12,17–24,28,29]:

$$P = P_{es} + P_{ed} + P_h + P_{fl} + \ldots \quad (1)$$

For surface potentials $\psi_0 = \text{const} < 25$ mV, in the presence of 1 : 1 electrolyte in concentration C_1, the P_{es} is [32]:

$$P_{es} = 64 C_1 RT \tanh^2(\phi/4)\, e^{-\kappa d_w} \quad (2)$$

and in the presence of 1 : 2 electrolyte in concentration C_2

$$P_{es} = 432 C_2 RT \tanh^2\{0.25 \ln[(2e^{\phi} + 1)/3]\}\, e^{-\kappa d_w} \quad (3)$$

In Eqns. 2 and 3 $\phi = F\psi_0/RT$ (ψ_0 is the electrostatic surface potential), κ is the reciprocal Debye length, d_w is the intermembrane separation, R, T, and F have their usual meanings. In the presence of both 1:1 and 1:2 electrolytes P_{es} is the sum of Eqns. 2 and 3. P_h and P_{ed} are defined as [5–7]:

$$P_h = P_0 e^{-d_w/\lambda} \tag{4}$$

$$P_{ed} = -\frac{H}{6\pi}\left[d_w^{-3} - 2(d_w + d_l)^{-3} + (d_w + 2d_l)^{-3}\right] \tag{5}$$

where P_0 is the hydration coefficient, λ is the decay constant of hydration pressure, H is the Hamaker constant, d_l is the membrane thickness. Here we restrict ourselves to the consideration of the electrostatic, electrodynamic, and hydration pressures. The free energy of interaction is:

$$G(d_w) = \int_{d_w}^{\infty} P\, dd_w \tag{6}$$

The geometry of lamellar structure in the absence of excess water predicts the following relations [6]:

$$Ad = 2(v_l + nv_w);\ d_l = d - d_w = 2v_l/A \tag{7}$$

where A is the cross-sectional area per lipid molecule, v_l and v_w are the molecular volumes of the lipid and water, respectively, n is the water/lipid molar ratio, d is the repeat spacing.

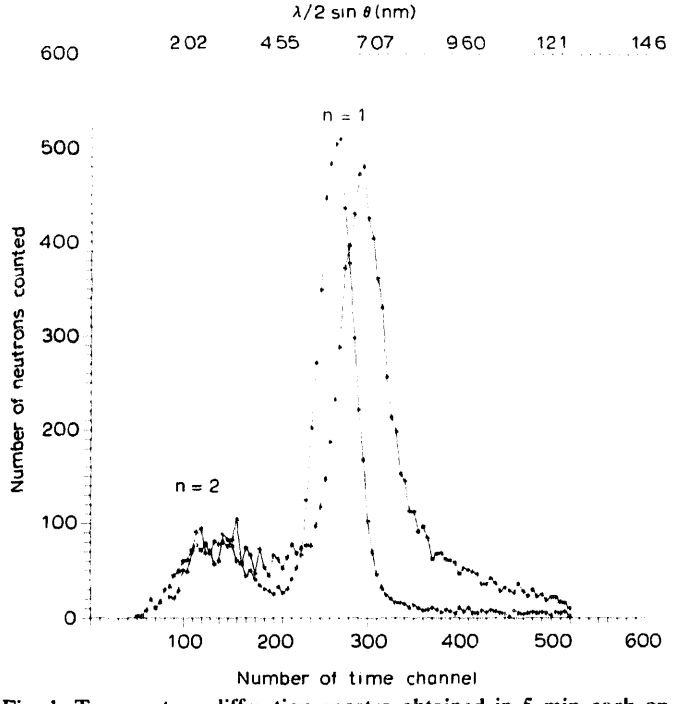

Fig. 1. Two neutron diffraction spectra obtained in 5 min each on samples containing 10 mg DPPC plus 20 μl ^2H_2O solution of 9 mM NaCl and 6.65 mM Tris-HCl (pH 7.4) at 20°C (left spectrum) and 48°C (right spectrum). Each point represents the sum of neutrons counted in five adjacent time channels. For further details see Materials and Methods.

Results

Fig. 1 represents two neutron diffraction spectra demonstrating that the first-order diffraction peaks were sharp enough to allow the repeat spacings to be determined with high certainty.

Depicted in Fig. 2 are the experimental curves of the temperature-dependence of DPPC lamellar repeat spacing in the presence of 6.65 mM Tris-HCl (pH 7.4) and varying concentrations of NaCl in the aqueous phase. These data indicate that the repeat spacing increases from 6.4 to 7.0–7.3 nm at about 35 °C, which is the temperature of the 'pretransition' (T_p) of DPPC from the gel to intermediate (or ripple) phase [33], and decreases to 6.5–6.8 nm at 40–42 °C, corresponding to the temperature of the 'main' transition (T_m) from ripple to liquid-crystalline phase [33]. These temperature-dependence curves are typical for phosphatidylcholine bilayers in the presence of simple salts and are in quantitative agreement with results obtained on DPPC [34,35].

Enhancement of NaCl concentration has no effect on d in the solid phase whereas d increases with decreasing ionic strength in the fluid phase, i.e., the liquid-crystalline membranes seem to be charged in contrast to gel-phase membranes. This may be accounted for by augmented negative surface potential of phosphatidylcholine bilayers in the fluid phase, as detected previously [3,25].

As seen from Fig. 3, increasing concentrations of $NaClO_4$ in the aqueous phase both in the absence and presence of 100 mM $CaCl_2$ cause marked deviations of the temperature dependence of the repeat spacing from the characteristic pattern. In the absence of $CaCl_2$ (Fig. 3A), the increase in $NaClO_4$ concentration results in an initial elevation and further reduction in the repeat spacing, while in the presence of 100 mM $CaCl_2$ (Fig. 3B) $NaClO_4$ gradually decreases the repeat spacing.

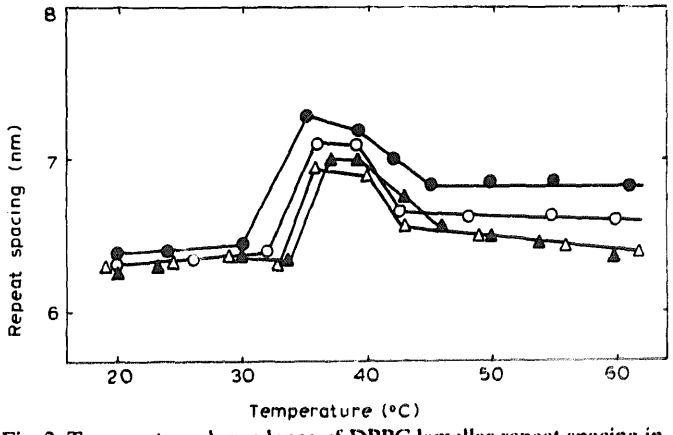

Fig. 2. Temperature-dependence of DPPC lamellar repeat spacing in the absence (●) and presence of 27 mM (○), 166 mM (△), and 665 mM NaCl (▲) in the aqueous phase containing 6.65 mM Tris-HCl (pH 7.4) at ^2H_2O/DPPC molar ratio of 81:1.

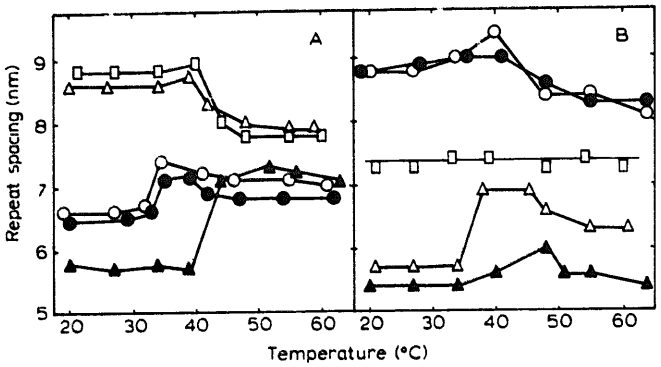

Fig. 3. Temperature-dependence of DPPC lamellar repeat spacing in the absence (A) and presence of 100 mM $CaCl_2$ (B) in the aqueous phase containing $NaClO_4$ in concentrations (mM): 1 (●), 9 (○), 83 (□), 116 (△), and 665 (▲). The medium contained 6.65 mM Tris-HCl (pH 7.4). The ^2H_2O/DPPC molar ratio was 81 : 1.

Data on the influence of NaCl, $NaClO_4$, and $CaCl_2$ on DPPC lamellar repeat spacing for both solid (20°C) and fluid bilayers (55°C) are presented in Figs. 4 and 5. The absence of more or less pronounced dependence of d on NaCl concentration (Fig. 4, curves 1, 2) indicates that NaCl does not affect DPPC lamellar structure and/or interactions, while the effect of $NaClO_4$ is appreciable (Fig. 4, curves 3, 4, and Fig. 5). The initial elevation of the repeat spacing as $NaClO_4$ concentration increases (Fig. 4, curves 3, 4) is most likely to be resulted from the adsorption of ClO_4^- anions to phosphatidylcholine bilayers and creation of negative surface potential, as demonstrated earlier [25,26], which gives rise to electrostatic interlamellar repulsion and additional swelling of the system. The impetuous reduction of d at higher (> 0.1–0.3 M) $NaClO_4$ concentrations (Fig. 4, curves 3, 4) might be governed by diverse mechanisms: (i) saturation of ClO_4^- adsorption and electrostatic screening of the surface charge by counter-ions (Na^+) at high ionic strengths [25,26], (ii) perturbation of the structure of membrane-bound water by ClO_4^- ions owing to their chaotropic nature [27], and (iii) decrease in membrane thickness caused by high concentrations of chaotropic anions [36,37].

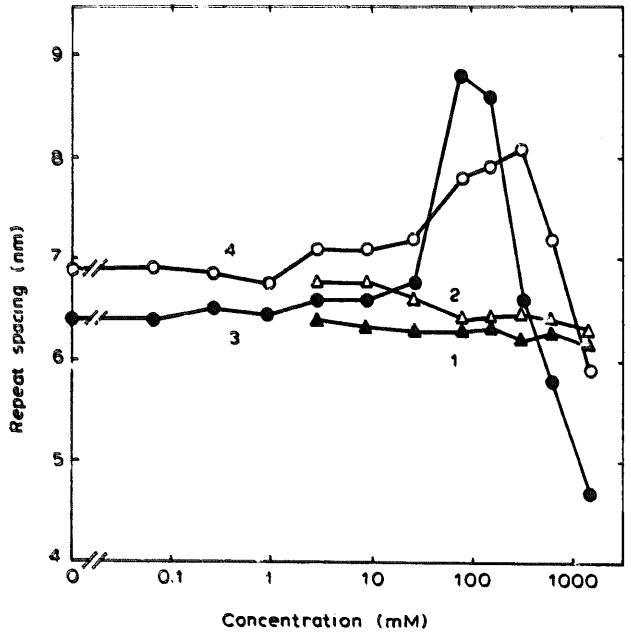

Fig. 4. Dependence of the repeat spacing of DPPC lamellar structure in heavy water on concentration of NaCl (curves 1, 2) and $NaClO_4$ (curves 3,4) in the aqueous phase containing 6.65 mM Tris-HCl (pH 7.4) at ^2H_2O/DPPC molar ratio of 81:1. Curves 1 and 3 correspond to 20°C, curves 2 and 4 correspond to 55°C.

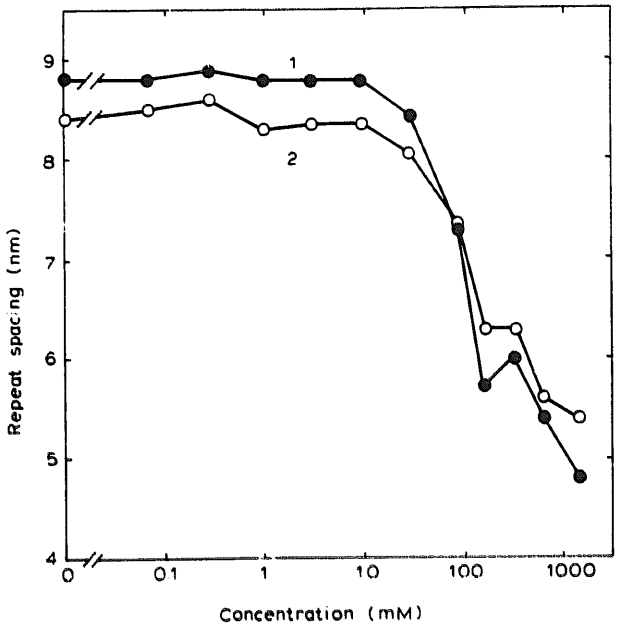

Fig. 5. Dependence of DPPC lamellar repeat spacing on $NaClO_4$ concentration in the presence of 100 mM $CaCl_2$ at 20°C (curve 1) and 55°C (curve 2). Otherwise as in Fig. 4.

In the presence of Tris-HCl buffer only, the DPPC lamellar repeat distance is 6.4 and 6.9 nm at 20 and 55 °C, respectively (Figs. 2, 4). Addition of 100 mM $CaCl_2$ to the aqueous phase leads to an increase in d to 8.4–8.8 nm (Fig. 5). This effect is in good agreement with the data of Inoko et al. [28] and Lis et al. [6] and evidently is accounted for by electrostatic repulsion between juxtaposed bilayers due to Ca^{2+}adsorption-induced positive surface potential. Increase in $NaClO_4$ concentration in the presence of 100 mM $CaCl_2$ is followed by progressive lowering of the repeat spacing. Reduction in d sets in at ≈ 10 mM $NaClO_4$ (Fig. 5), which could be explained by ClO_4^- binding and decrease in the positive surface potential of the bilayers, congruously with the increase in d at 10–30 mM $NaClO_4$ in the absence of $CaCl_2$ (Fig. 4, curves 3, 4). Further decrease in the repeat spacing at higher $NaClO_4$ concentrations might be interpreted invoking the three above mentioned mechanisms, i.e., electrostatic screening of the surface charge, reduction in hydration forces by ClO_4^- ions, and membrane thinning at high concentrations of chaotropic ions.

To distinguish between these possibilities first of all the membrane thickness in media of various ionic

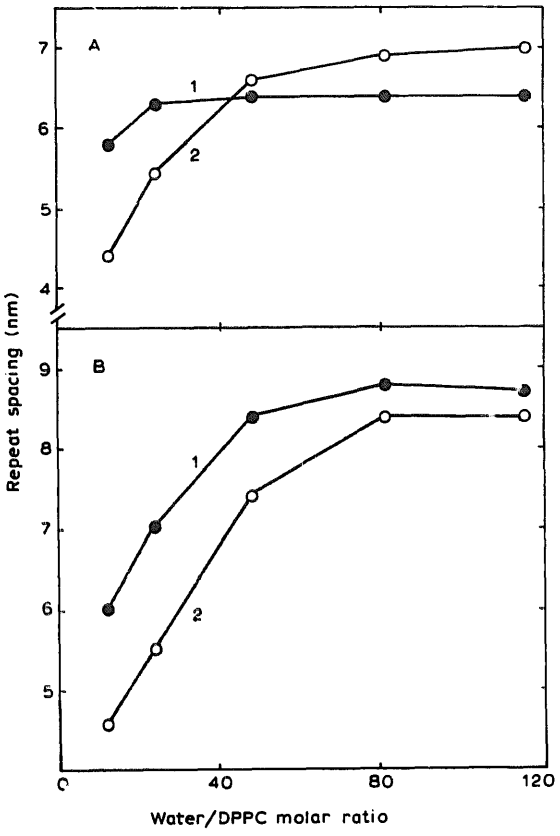

Fig. 6. Dependence of DPPC lamellar repeat spacing on ^2H_2O/DPPC molar ratio in the absence (A) and presence of 100 mM $CaCl_2$ (B) in the aqueous phase containing 6.65 mM Tris-HCl (pH 7.4). Filled and open circles refer to 20 and 55°C, respectively.

composition should be measured. Fig. 6 demonstrates that decrease in ^2H_2O/DPPC molar ratio is followed by remarkable reduction of the repeat spacing, which is undoubtedly due to the fact that at low water/lipid ratios no excess water is present to allow the system to swell sufficiently (see Refs. 6, 11, 12 and 35). Hence, Eqns. 7 can be applied to derive both the membrane thickness (d_l) and area per lipid molecule (A). Summarized in Table I are the parameters d_l and A determined through Eqns. 7 using the values of the repeat spacing at ^2H_2O/DPPC = 12:1 (Fig. 6) and the molecular volumes of $v_l = 1.1427$ nm^3 and $v_w = 0.03008$ nm^3 at 20°C and $v_l = 1.2317$ nm^3 and $v_w = 0.03051$ nm^3 at 55°C [30,31]. Values of the bilayer thickness in both gel and liquid crystalline phases of DPPC, shown in Table I, demonstrate no dependence on the presence of $CaCl_2$ and agree with the data deduced from X-ray diffraction with an accuracy of ±0.2 nm [5–7,9,12,22,34,35]. Note that the DPPC bilayer thickness and area per molecule found here at ^2H_2O/DPPC molar ratio of 12:1 (25 wt.% water) coincide with the respective parameters evaluated at equilibrium with excess water [6,7,12] which is in line with the findings that both d_l and A are almost independent of water content at ≥ 25 wt.% water [5,6,9,22,38]. McIntosh and Simon [22] pointed out that the DPPC bilayer thickness remained constant as the membranes were moved from their equilibrium separation to within 0.2–0.4 nm of each other.

The values of P_{es} at different NaCl concentrations (Fig. 2) were calculated through Eqn. 2 taking into account small negative surface charge densities of DPPC, determined previously as $\sigma_0 = -1.05$ and -1.89 mC/m^2 for solid and fluid membranes, respectively [26]. In the presence of 100 mM $CaCl_2$ and absence of $NaClO_4$ (Fig. 5), the electrostatic pressure was derived from a combination of Eqns. 2 and 3 with reference to Ca^{2+}-binding-induced surface charge apart from σ_0. The binding of Ca^{2+} ions to DPPC bilayers was described using the intrinsic binding constants of $K = 440$ and 190 M^{-1} and binding site densities of $N = 0.14$ and 0.13 nm^{-2} at 20 and 55°C, respectively, as found earlier [26]. Furthermore, the values of hydration pressure, P_h, were evaluated by Eqn. 4 using $P_0 = 10^{8.83}$ N/m^2, $\lambda = 0.20$ nm for solid bilayers and $P_0 = 10^{9.99}$ N/m^2, $\lambda = 0.22$ nm for fluid membranes, as reported by Lis et al. [7], and intermembrane separations deduced from corresponding d and d_l values determined here (d_l was averaged as 4.4 and 3.4 nm for solid and fluid films, respectively). The following Hamaker constants were then found combining Eqns. 2–5 with the condition of equilibrium, $P_{es} + P_{ed} + P_h = 0$: $H = (6.58 \pm 0.7) \cdot 10^{-21}$ J and $H = (6.52 \pm 0.8) \cdot 10^{-21}$ J for different NaCl concentrations (Fig. 4), and $H = 2.71 \cdot 10^{-21}$ J and $H = 1.02 \cdot 10^{-21}$ J in the presence of 100 mM $CaCl_2$ (Fig. 5) at 20 and 55°C, respectively.

The curves in Fig. 7, simulated with the use of Eqns. 1, 2, 4–6 (regarding P as a sum of P_{es}, P_{ed}, and P_h) and parameters corresponding to 20°C, show that in

TABLE I

The repeat spacing (d), membrane thickness (d_l), interbilayer separation (d_w), and cross-sectional area per DPPC molecule (A) at ^2H_2O/DPPC molar ratio of 12:1

Salt added to 6.65 mM Tris-HCl	T (°C)	d (nm)	d_l (nm)	d_w (nm)	A (nm^2)
–	20	5.8	4.31	1.49	0.52
–	55	4.4	3.39	1.01	0.73
100 mM $CaCl_2$	20	6.0	4.56	1.44	0.50
100 mM $CaCl_2$	55	4.6	3.55	1.05	0.70

the presence of 40 mM 1:1 electrolyte at $\psi_0 < 9$ mV the $G(d_w)$ curves exhibit a single ('primary') minimum, corresponding to 2 nm equilibrium separation and determined by a balance between P_h and P_{ed}. An increase in ψ_0 to 10 and then to 11 mV leads to the appearance of an additional ('secondary') minimum, due to the equilibration between P_{es} and P_{ed} (P_h is insignificant at $d_w \geq 4$ nm) and, correspondingly, an energy barrier between the two minima owing to the electrostatic repulsion. These findings imply that the pronounced rise in lamellar repeat spacing when $NaClO_4$ concentration is increased from 27 to 83 mM at 20°C (Fig. 4, curve 3) might be explained by an increase in ψ_0 in the range 9–11 mV, resulted from ClO_4^- adsorption, which would cause a shift of the system from the 'primary' to the 'secondary' minimum. The results of the preliminary electrophoresis experiments performed by Yuri Ermakov provided confirmative evidence for this inference showing that the increase of $NaClO_4$ concentration from 10 to 55 mM caused an elevation of the zeta potential of DPPC liposomes from −8 to −15 mV at 20°C in the presence of 5 mM Tris-HCl (pH 7.4).

As demonstrate the curves of Fig. 8 (A, B), constructed using corresponding parameters (found in this work and by Lis et al. [7]), in the presence of 80 mM 1:1 salt an increase of ψ_0 from 0 to 14 mV is predicted to raise the equilibrium interbilayer separation by ≈ 3.5 nm and by ≈ 1.6 nm at 20 and 55°C, respectively, i.e.,

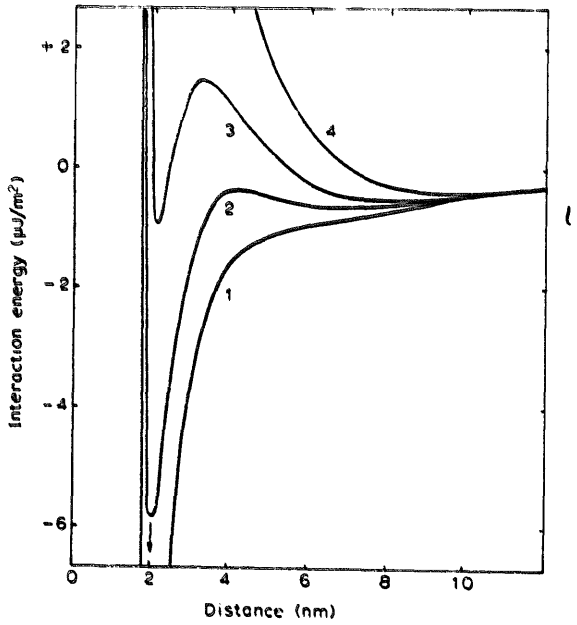

Fig. 7. Theoretical curves of the dependence of interaction free energy on intermembrane separation simulated by Eqns. 1, 2, 4–6 with the use of parameters: $C_1 = 40$ mM, $\kappa = 6.75 \cdot 10^8$ m^{-1}, $T = 293$ K, $P_0 = 10^{8.83}$ N/m^2, $\lambda = 0.2$ nm, $H = 6.58 \cdot 10^{-21}$ J, $d_1 = 4.4$ nm. The total disjoining pressure was assumed to be composed of P_{es}, P_{ed}, and P_h. The curves 1–4 correspond to the surface potentials of $\psi_0 = 9$, 10, 11, and 12 mV, respectively. The down-faced arrow indicates the position of minimum of the curve 1.

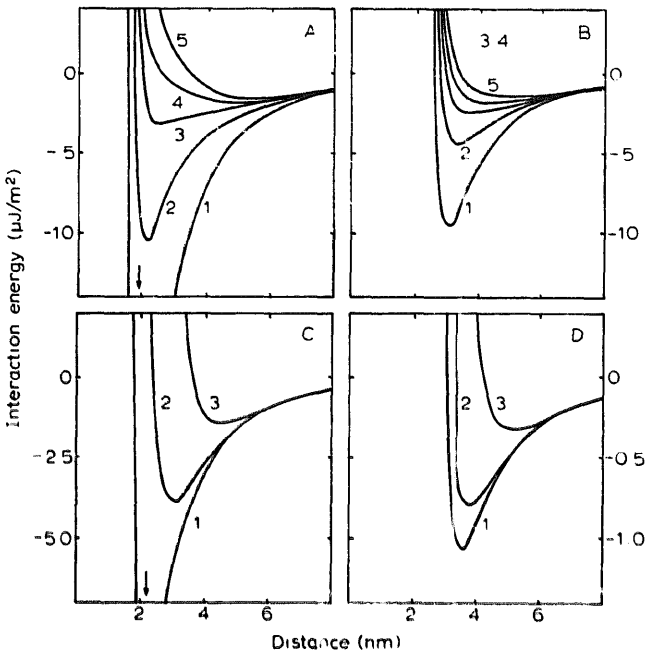

Fig. 8. Dependence of interaction free energy on intermembrane separation simulated through Eqns. 1–6 using parameters: $C_1 = 80$ mM, $C_2 = 0$ (A, B); $C_1 = 1.5$ M, 0.2 M, and 6.65 mM (curves 1, 2, 3, respectively), $C_2 = 0.1$ M (C, D); $T = 293$ K (A, C) and 328 K (B, D); the curves 1–5 of the panels A and B correspond to $\psi_0 = 3$, 10, 12, 13, and 14 mV, respectively; the curves 1, 2, 3 correspond to $\psi_0 = 12.3$, 23.7, and 29.34 mV (C) and 13.05, 22.6, and 27.6 mV (D), respectively. The surface potentials corresponding to the curves of panels C and D were estimated using the intrinsic constants of Ca^{2+} binding to DPPC bilayers as 440 and 190 M^{-1} and binding site densities of 0.14 and 0.13 nm^{-2} at 20 and 55°C, respectively (see Ref. 26) taking into account corresponding ionic strengths. The Hamaker constants and membrane thicknesses presented in the text and Table I were used. The parameters P_0 and λ were taken from Ref. 7 as: $P_0 = 10^{8.83}$ N/m^2, $\lambda = 0.20$ nm at 20 °C and $P_0 = 10^{9.99}$ N/m^2, $\lambda = 0.22$ nm at 55°C.

less pronounced changes of the repeat spacing are expected in the case of fluid bilayers, as detected experimentally (cf. curves 3 and 4, Fig. 4).

Calculations through the Gouy-Chapman-Stern theory using the parameters of Ca^{2+} binding to DPPC bilayers from Ref. 26 (see the legend to Fig. 8) showed that in the presence of 100 mM $CaCl_2$ the increase of the ionic strength from 6.65 mM (Tris-HCl only) to 1.5 M will reduce the membrane surface potential from ≈ 30 to ≈ 13 mV, which, as shown in Fig. 8 (C, D), predicts a decrease of intermembrane separation from 4.4 to 2.2 nm at 20 °C and from 5.0 to 3.6 nm at 55 °C. Taking into account corresponding values of the bilayer thickness (4.4 and 3.4 nm at 20 and 55°C), it becomes clear that the electrostatic screening of the Ca^{2+}-induced surface potential would lower the repeat spacing from 8.8 to 6.6 nm at 20°C and from 8.4 to 7.0 nm at 55°C. Data of Fig. 5 show, however, that the decrease in d considerably exceeds that expected from Debye screening. Moreover, it can easily be shown using Eqns. 1–6 that at high ionic strengths the equilibrium separation is largely insensitive to the surface

potential because the range of the action of electrostatic forces becomes shorter, owing to short Debye lengths, than that of much more stronger hydration forces. Even if the positive surface potential was completely vanished at 1.5 M $NaClO_4$, due to ClO_4^- binding, the repeat distance could not fall below 6.6–7.0 nm provided the hydration coefficient and membrane thickness remain constant. Nor the repeat distance in the absence of $CaCl_2$ could diminish so sharply as detected at $\approx$ 1 M $NaClO_4$ (Fig. 4, curves 3, 4) if the effect was due solely to Debye screening. The latter is validated, apart from the theoretical predictions, by the fact that d is higher in the presence of 1.5 M NaCl than $NaClO_4$, especially in the case of solid membranes (Fig. 4). These results strongly suggest that the pronounced decrease in the lamellar repeat spacing at high $NaClO_4$ concentrations is accounted for by deviations of other parameters than the surface potential, presumably the hydration coefficient and/or membrane thickness.

To check this anticipation the bilayer thickness has been evaluated in the presence of 1.5 M $NaClO_4$. Decrease in the water/lipid molar ratio up to 12:1 progressively reduces the lamellar repeat spacing (Fig. 9) which indicates the absence of the excess water. This allows the Eqns. 7 to be used to obtain the parameters d_l, d_w, and A (Table II). Then, recalling that the membrane thickness does not depend on water content at DPPC wt.% from 30 to 75 [5,6,38] (n = 12 and 81 correspond to DPPC wt.% of 75 and 31, respectively), intermembrane separations at n = 81 were deduced from experimental values of d at 1.5 M $NaClO_4$ (Figs. 4, 5) and values of d_l at n = 12 (Table II). In the presence of 1.5 M monovalent salt the Debye length is $\approx$ 0.25 nm, so that the electrostatic pressure at $d_w \approx$ 1.5 nm could be neglected and the condition for equilibrium presented as $P_h = P_{cd}$. This relation was used together with Eqns. 4 and 5 to find the hydration coefficient, P_0, in the presence of 1.5 M $NaClO_4$ at ^2H_2O/DPPC = 81:1 (Table II). The parameters λ = 0.2 and 0.22 nm were used for solid and fluid DPPC bilayers, respectively [7]. The respective values of d_w, d_l, and H were used as evaluated in this work.

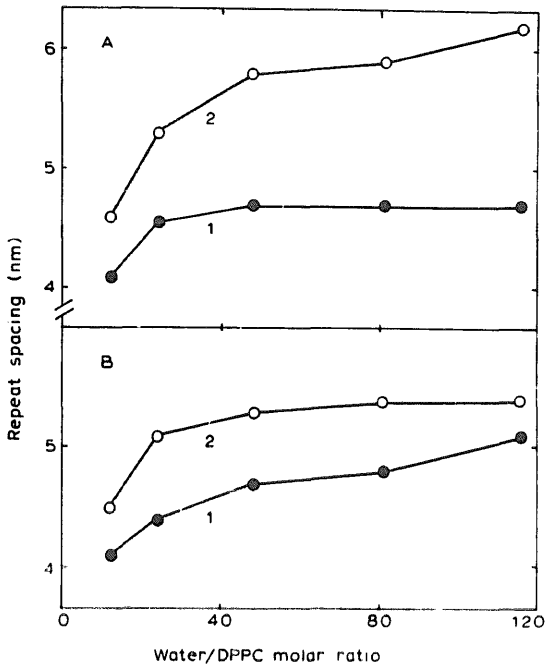

Fig. 9. Dependence of the DPPC lamellar repeat spacing on ^2H_2O/DPPC molar ratio in the presence of 1.5 M $NaClO_4$ and 6.65 mM Tris-HCl (A) and 1.5 M $NaClO_4$, 0.1 M $CaCl_2$, and 6.65 mM Tris-HCl (B). The curves 1 and 2 correspond to 20 and 55°C, respectively.

The hydration coefficient of DPPC lamellae was estimated as $(3.4–6.7) \cdot 10^8$ N/m^2 in the gel phase [7,9,23] and $9.8 \cdot 10^9$ N/m^2 in the fluid phase [7]. The values of P_0 evaluated here amount, in the presence of 1.5 M $NaClO_4$, to $2.1 \cdot 10^8$ and $9.7 \cdot 10^8$ N/m^2 at 20 and 55°C, respectively (Table II). This implies that 1.5 M $NaClO_4$ causes a lowering of the hydration of DPPC bilayers. Taking into account that NaCl up to 1.5 M does not affect Significantly the lamellar repeat distance (Fig. 4), it becomes clear that the decrease in P_0 is induced by the chaotropic ClO_4^- anions and is very likely to be resulted from the disruption of the structure of membrane-bound water owing to the structure-breaking nature of ClO_4^- ions [27]. The values of P_0 in the presence of 100 mM $CaCl_2$ (Table II) demonstrate that Ca^{2+} ions induce additional dehydration of lipid bilayers, which is a widely recognized phenomenon [1,2,18].

TABLE II

Some parameters of DPPC membrane structure and interactions in the presence of 1.5 M $NaClO_4$ and 6.65 mM Tris-HCl (pH 7.4) at ^2H_2O/DPPC molar ratios of 12:1 and 81:1

Salt added to 1.5 M $NaClO_4$ and 6.65 mM Tris-HCl	T (°C)	n = 12			n = 81	
		d_l (nm)	d_w (nm)	A (nm^2)	d_w (nm)	P_0 (N/m^2)
–	20	3.14	0.96	0.73	1.56	$2.10 \cdot 10^8$
–	55	3.57	1.03	0.69	2.33	$9.70 \cdot 10^8$
100 mM $CaCl_2$	20	3.14	0.96	0.73	1.66	$1.17 \cdot 10^8$
100 mM $CaCl_2$	55	3.49	1.01	0.71	1.91	$4.22 \cdot 10^8$

Discussion

The variations of DPPC lamellar repeat spacing at the temperatures of pretransition (gel-to-ripple) and main phase transition (ripple-to-fluid), presented in Fig. 2, agree quantitatively with the data of others [34,35]. The enhancement of d at T_p is most likely to be resulted from interbilayer repulsion due to increased thermal-mechanical fluctuations of bilayers in the ripple phase [19,21,34], the amplitude of which reaches ≈ 2.5 nm [34]. The interpretation for increased repeat distance of fluid lamellar phase (55°C) as compared to the gel phase (20 °C) is not unambiguous. The thermal undulations might again be responsible for this [10,17,19,20,22]. However, phospholipid bilayers in the fluid phase were shown to be repelled from each other more strongly than those in the gel phase even when the lipid was immobilized on mica sheets [17]. Evans and Parsegian [21] concluded that the decrease in the equilibrium interbilayer separation at the fluid-to-solid transition was accounted for by reduction in membrane hydration rather than by suppressed fluctuations. This inference is consistent with the findings of Lis et al. [7] that both P_0 and λ increased at DPPC chain melting, implying that greater hydration forces operate between fluid membranes at any separation, but accords only partly with the results of McIntosh and Simon [22] reporting higher P_0 but shorter λ for solid DPPC bilayers as compared to fluid egg phosphatidylcholine membranes so that at $d_w > 1.5$ nm P_h becomes stronger in the latter case and the conflict disappears. Taking into account these considerations and the fact that equilibrium intermembrane separation in phosphatidylcholine/water systems is ≥ 2 nm [5,7,9–12] the increase in d at gel-to-liquid-crystalline phase transition of DPPC (Fig. 2) could be interpreted in terms of increase in hydration repulsion at the bilayer fluidization.

The values of d in the presence of 100 mM $CaCl_2$ and absence of $NaClO_4$ (Fig. 5) agree with those measured under similar conditions [6,28]. These augmented repeat spacings (as compared to those in the absence of Ca^{2+}) have been ascribed to Ca^{2+}-adsorption-induced electrostatic repulsion, equilibrated by van der Waals attraction [6]. The fact that at low $NaClO_4$ concentrations the repeat spacing is greater for solid bilayers than for fluid films (Fig. 5) could be explained by weaker Ca^{2+} binding to fluid DPPC bilayers than to solid membranes [26].

The values of d_1 and A estimated in the presence of 1.5 M $NaClO_4$ (Table II) strongly suggest that $NaClO_4$ induces the formation of interdigitated phase of DPPC membranes in the solid state. In fact, the thickness of DPPC membranes with interdigitated (or interpenetrated) acyl chains, detected at 20–25 °C in the presence of 1 M KSCN [36,37] or 1,2,3-heptanetriol [9], was measured as 2.77 nm [36,37] and 3.0 nm [9], and the area per DPPC molecule was 0.78 nm^2 [9]. Note that the DPPC interdigitated phase was produced by 1 M SCN^- anions which resemble ClO_4^- by their chaotropic properties [27]. We measured the repeat spacing at ^2H_2O/DPPC = 81 (molar) in the presence of 665 mM NaSCN and obtained $d = 5.3$ and 7.0 nm at 20 and 55°C, respectively, indicating the similarity of the effects of SCN^- and ClO_4^- ions on DPPC. On the other hand, the values of the repeat spacing at different concentrations of Na_2SO_4 (not shown) were close to those in the presence of NaCl (Fig. 3), implying that neither Cl^- nor SO_4^{2-} affect the phospholipid membrane lamellar structure. Interestingly, the organic anion 1-anilino-8-naphthalene sulfonate at high concentrations caused a 1.5 nm reduction of the thickness of phospholipid membranes [39], indicative of interdigitated phase formation. These data provide evidence that the formation of interdigitated phase is caused by chaotropic, or structure-breaking ions, possessing low charge density, whereas kosmotropic *, or structure-making ions, are not effective.

The effect of chaotropic ions on membrane structure could be interpreted taking into consideration that the interdigitated phase assumes contact of water, to a certain extent, with the terminal hydrophobic groups of the lipid acyl chains and, on the other hand, that 'chaotropic ions favor the transfer of apolar groups to water' [40]. In the case of melted acyl chains, water is expected to penetrate deeper into the membrane hydrophobic core, which is thermodynamically unfavorable, therefore interdigitated phase is prevented for fluid membranes.

Acknowledgements

We are so much thankful to Yuri Ermakov for electrophoresis experiments, as well as to Sidney Simon, Peter Rand and Adrian Parsegian for fruitful discussions and comments.

References

1 Rand, R.P. Das, S. and Parsegian, V.A. (1985) Chem. Script. 25, 15–21.
2 Rand, R.P. and Parsegian, V.A. (1986) Annu. Rev. Physiol. 48, 201–212.
3 Tatulian, S.A. (1987) Biochim. Biophys. Acta 901, 161–165.
4 Hoekstra, D. and Wilschut, J. (1989) in Water Transport in Biological Membranes (Benga, G., ed.), pp. 143–176, CRC, Boca Raton.
5 Rand, R.P. (1981) Annu. Rev. Biophys. Bioeng. 10, 277–314.

* The terms 'kosmotropic' and 'chaotropic' originate from Greek κοσμος (order) and χαος (disorder).

6 Lis, L.J., Parsegian, V.A. and Rand, R.P. (1981) Biochemistry 20, 1761–1770.
7 Lis, L.J., McAlister, M., Fuller, N., Rand, R.P. and Parsegian, V.A. (1982) Biophys. J. 37, 657–666.
8 Derjaguin, B.V. and Churaev, N.V. (1986) in Fluid Interfacial Phenomena (Croxton, C.A., ed.), pp. 663–738, Wiley, Chichester.
9 Simon, S.A., McIntosh, T.J. and Magid, A.D. (1988) J. Colloid Interface Sci. 126, 74–83.
10 Simon, S.A. and McIntosh, T.J. (1989) Proc. Natl. Acad. Sci. USA 86, 9263–9267.
11 Rand, R.P., Fuller, N., Parsegian, V.A. and Rau, D.C. (1988) Biochemistry 27, 7711–7722.
12 Rand, R.P. and Parsegian, V.A. (1989) Biochim. Biophys. Acta 988, 351–376.
13 Curtis, A.S.G., Campbell, J. and Shaw, F.M. (1975) J. Cell Sci. 18, 347–356.
14 Curtis, A.S.G., Shaw, F.M. and Spires, V.M.C. (1975) J. Cell Sci. 18, 357–373.
15 Curtis, A.S.G., Chandler, C. and Picton, N. (1975) J. Cell Sci. 18, 375–384.
16 Schaeffer, B.E. and Curtis, A.S.G. (1977) J. Cell Sci. 26, 47–55.
17 Marra, J. and Israelachvili, J. (1985) Biochemistry 24, 4608–4618.
18 Marra, J. (1986) Biophys. J. 50, 815–825.
19 Helfrich, W. (1978) Z. Naturforsch. 33a, 305–315.
20 Harbich, W. and Helfrich, W. (1984) Chem. Phys. Lipids 36, 39–63.
21 Evans, E.A. and Parsegian, V.A. (1986) Proc. Natl. Acad. Sci. USA 83, 7132–7136.
22 McIntosh, T.J. and Simon, S.A. (1986) Biochemistry 25, 4058–4066.
23 Marsh, D. (1989) Biophys. J. 55, 1093–1100.
24 Parsegian, V.A. and Rau, D.C. (1984) J. Cell Biol. 99, 196s-200s.
25 Tatulian, S.A. (1983) Biochim. Biophys. Acta 736, 189–195.
26 Tatulian, S.A. (1987) Eur. J. Biochem. 170, 413–420.
27 Collins, K.D. and Washabaugh, M.W. (1985) Q. Rev. Biophys. 18, 323–422.
28 Inoko, Y., Yamaguchi, T., Furuya, K. and Mitsui, T. (1975) Biochim. Biophys. Acta 413, 24–32.
29 Ohshima, H., Inoko, Y. and Mitsui, T. (1982) J. Colloid Interface Sci. 86, 57–72.
30 Nagle, J.F. and Wilkinson, D.A. (1978) Biophys. J. 23, 159–175.
31 Chemical Handbook (1962) Vol. 1, p. 547, Goskhimizdat, Moscow (in Russian).
32 Derjaguin, B.V., Churaev, N.V. and Muller, V.M. (1985) in Surface Forces (Shchukin, E.D., ed.) Nauka, Moscow (in Russian).
33 Mabrey, S. and Sturtevant, J.M. (1976) Proc. Natl. Acad. Sci. USA 73, 3862–3866.
34 Parsegian, V.A. (1983) Biophys. J. 44, 413–415.
35 Lvov, J.M., Mogilevskij, L.J., Fejgin, L.A., Gyorgyi, S., Ronto, Gy., Thompson, K.K. and Sugar, I.P. (1986) Mol. Cryst. Liq. Cryst. 133, 65–73.
36 Cunningham, B.A., Lis, L.J. and Quinn, P.J. (1986) Mol. Cryst. Liq. Cryst. 141, 361–367.
37 Cunningham, B.A. and Lis, L.J. (1986) Biochim. Biophys. Acta. 861, 237–242.
38 Janiak, M.J., Small, D.M. and Shipley, G.G. (1979) J. Biol. Chem. 254, 6068–6078.
39 Lesslauer, W., Cain, J. and Blasie, J.K. (1971) Biochim. Biophys. Acta 241, 547–566.
40 Hatefi, Y. and Hanstein, W.G. (1969) Proc. Natl. Acad. Sci. USA 62, 1129–1136.